Study of Leaf-shaped Element Bowtie Antenna with Flat Reflector for UWB Applications

Michitaka AMEYA [1], Manabu YAMAMOTO [1], Toshio NOJIMA [1], Kiyohiko ITOH [2]
[1] *Graduate School of Information Science and Technology, Hokkaido University*
N14, W9, Kita-ward, Sapporo, 060-0814 Japan, {ameya,yamamoto,nojima}@emwtinfo.ice.eng.hokudai.ac.jp
[2] *Tomakomai National College of Technology*
Nishikioka 443, Tomakomai, 059-1275 Japan, itoh@office.tomakomai-ct.ac.jp

Abstract

In this paper, we propose a novel bowtie antenna using leaf-shaped radiating elements for UWB applications. This antenna has unidirectional radiation patterns over the frequency range of 3.0 to 10.5 GHz. *The actual gain in the maximum radiation direction is above 5* dBi *in the UWB frequency band. From the evaluation of cross-correlation between source pulse and received pulse waveforms, it is observed that the waveform distortion caused by this antenna is relatively small.*

1. Introduction

Ultra-wideband (UWB) communication systems have attracted considerable attention in recent years. In impulse-based UWB communications, if correlation detection is used as the demodulation scheme, waveform distortions of transmitted and received pulses caused by antennas induce degradations of the communication performance[1]. In order to avoid these degradations, it is necessary that radiation characteristics of the antenna be constant over the wide frequency range.

Since the FCC announced that it would allow the unlicensed use of the bandwidth of 3.1 to 10.6 GHz[2], many UWB antennas have been studied[3]–[7]. Schantz proposed various new designs such as magnetic slot antennas[3] and planar elliptical dipole antennas[4]. Chen et al. investigated the characteristics of a few types of square dipole antennas[5] and also proposed the bi–arm rolled monopole[6]. The authors have recently proposed an omnidirectional UWB printed dipole antenna[7]. The antenna is similar to a bowtie antenna. The radiating element of the antenna is leaf-shaped. The radiation patterns of the antenna are omnidirectional in 3.0–10.5 GHz. The waveform distortion caused by the antenna is very small.

All these antennas have omnidirectional radiation patterns and the gains of these antennas are relatively low, about 0–3 dBi. When these omnidirectional antennas were attached to walls or metals, it is suspected that the antenna performances can be degraded due to the omnidirectionality. In order to avoid the degradation of the antenna performance, we considered placing a flat reflector behind the leaf-shaped bowtie antenna. In addition, high gain UWB antenna permits us to realize higher speed communication and to reduce power consumption.

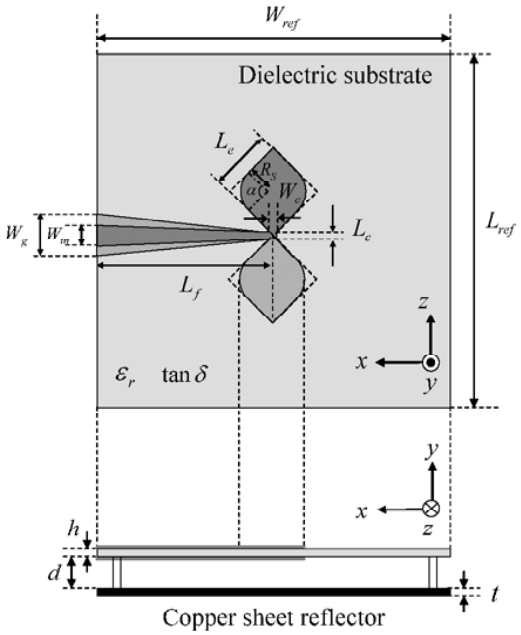

Fig. 1: Antenna Geometry and parameters when using the tapered microstrip line feed.

One of the most important topics in UWB antennas is the waveform distortion caused by antennas. There are a few works on the evaluation of the waveform distortion in terms of cross-correlation[8], [9]. In this paper, we proposed a novel UWB antenna and verified the validity of the proposed antenna by evaluating the waveform distortions.

In Section 2, we describe the antenna configuration of the proposed antenna. The antenna characteristics are investigated by comparing the experimental results with the FDTD results. Then, the results and discussion are described in Section 3. Finally, the conclusions of this work are given in Section 4.

2. Antenna Configuration

Antennas for UWB applications are required to have constant input impedance over the wide frequency range. The principle of self-complementarity[10] is a method for realizing constant impedance characteristics. Hence, we design the radiation

TABLE 1: ANTENNA PARAMETERS.

$W_{\rm ref}$[mm]	$L_{\rm ref}$[mm]	h[mm]	ε_r	$\tan\delta$
100	100	0.762	2.17	0.0009

R_s[mm]	α	L_e[mm]	d[mm]	t[mm]
7.1	90°	12	9	0.5

$W_{\rm in}$[mm]	W_g[mm]	L_f[mm]	W_c[mm]	L_c[mm]
2.4	12	50	0.2	0.2

elements of the printed dipole antennas based on the theory of self-complementarity. The ideal self-complementary antenna presupposes an infinite structure. Therefore, we need to truncate the infinite structure for designing practical radiating elements. As long as self-complementarity is maintained around the feeding point of the radiating elements, various kinds of shapes can be adopted for the truncated part of the radiating element.

In this paper, leaf-shaped elements are employed as shown in Fig. 1. Two leaf-shaped radiating elements are arranged on upper and lower surfaces of a dielectric substrate with thickness $h = 0.762$ mm, dielectric constant $\varepsilon_r = 2.17$, and $\tan\delta = 0.0009$@10 GHz. For simplicity, the reflector size $W_{\rm ref}$ and $L_{\rm ref}$ are both set to 100 mm and the substrate size is equal to the reflector size. The leaf shape is designed by rounding the corner of the square shape, and then the curvature radius of the rounded corner R_s is set to 7.1 mm. The element size L_e is set to 12 mm. These values are optimized for operating in the UWB band[7]. The separation d between the antenna and the reflector is set to 9 mm because the widest gain bandwidth was obtained at $d = 9$ mm. The leaf-shaped radiating elements are excited by a 50 mm tapered microstrip line. The width L_c of the feeding line at the center is set to 0.2 mm because the input impedance at the center of both radiating elements, which is calculated by using FDTD delta-gap feeding model, is about 150 Ω. This value is close to the input impedance of the self-complementary planar structure ($120\pi/2$). The width $W_{\rm in}$ of the feeding line at the input port is 2.4 mm for connecting to a 50 Ω SMA connector. A copper plate having a thickness of 0.5 mm is used as a reflector. The remaining parameters of the proposed antenna is shown in Table 1.

3. SIMULATION AND EXPERIMENTAL RESULTS

A. Reflection, Actual Gain, and Radiation Patterns

The frequency responses of the measured and calculated reflection coefficients (S_{11}) are illustrated in Fig.2. In order to evaluate the effect of the reflector on the input reflection, the reflection of the antenna without the reflector is also shown in the figure. As can be seen from this figure, the measured and calculated results are in good agreement. With the reflector, input reflection increases by about 4 dB in the frequency range less than 10 GHz.

The actual gain in the y direction as a function of frequency are plotted in Fig.3. To examine the effect of the feed line, the gain of the antenna using a delta-gap voltage source

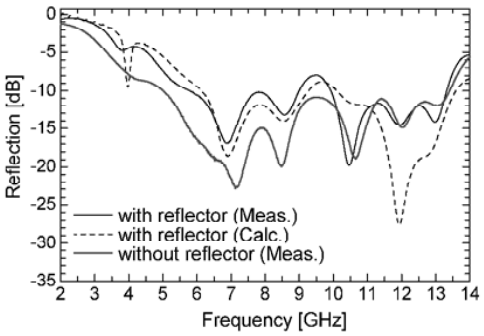

Fig. 2: Frequency response of the reflection coefficients.

is shown in the figure. The measured results coincide with the calculated results. The −3dB relative bandwidth of the measured gain is 80.3%. It is a reduction of 20.7% from the results of the delta-gap feed model. The reason for the decreasing bandwidth is due to the gain drops around 4 and 10 GHz. The delta-gap feed model has less than −30 dBi cross-polarization level in all frequency range. However, in the case of the tapered microstrip-line feed model, it was verified by measured and calculated results that the cross-polarization level around 4 GHz is higher than the level in other frequencies. Accordingly, the tapered microstrip-line acts as an antenna and does not transmit the power to the leaf-shaped radiating elements. The drop at around 10 GHz may be due to the increase of the reflection. The maximum gain is 8.2 dBi at 7.28 GHz in the measured results.

The radiation patterns in the azimuthal plane (xy plane) and the elevation plane (yz plane) are measured. Some of these results are shown in Figs.4 and 5. Although the pattern shape is a little disturbed at 10.5 GHz, unidirectional radiation patterns with small frequency dependence are obtained from 3.0 to 10.5 GHz. In the azimuthal plane, the half power beam width (HPBW) is 68°, 93°, 102°, 122°, and 129° in ascending order by the frequency (except 10.5 GHz). In the elevation plane, the HPBW is 49°, 57°, 58°, 58°, and 55°, respectively. Consequently, the beam width in the elevation plane is narrower than that in the azimuthal plane.

B. Transmission Characteristics

In order to investigate the transmission characteristics of the proposed antenna, the measurements of the transmission loss and group delay characteristics were conducted. We investigated the transmitting and receiving system using a pair of the proposed antennas, which are arranged with a separation of $d = 1$ m. To clarify variations of the transmission characteristics due to changing azimuthal angle, the measurements were performed at every 5° from $\phi_{\rm rx} = 0°$ to 355° ($\phi_{\rm rx}$ is the direction of the receiving antenna). The direction of the transmitting antenna is fixed at the maximum radiation direction ($\phi_{\rm tx} = 90°$). For comparison purposes, the measurements of the microstrip line (MSL) thin dipole antenna with reflector were also performed.

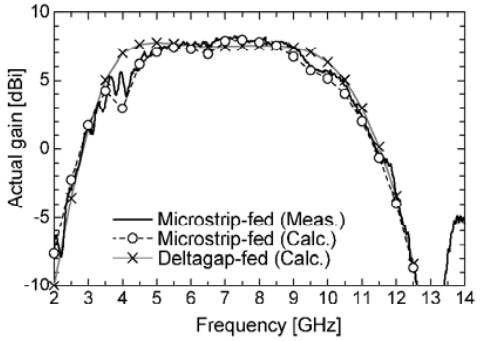

Fig. 3: Frequency response of the actual gain for the tapered microstrip line feed model and delta-gap feed model.

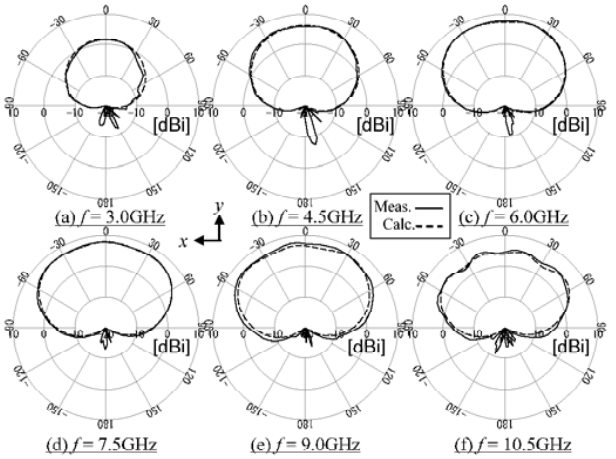

Fig. 4: Radiation patterns in xy plane at the frequency of 3.0, 4.5, 6.0, 7.5, 9.0 and 10.5 GHz.

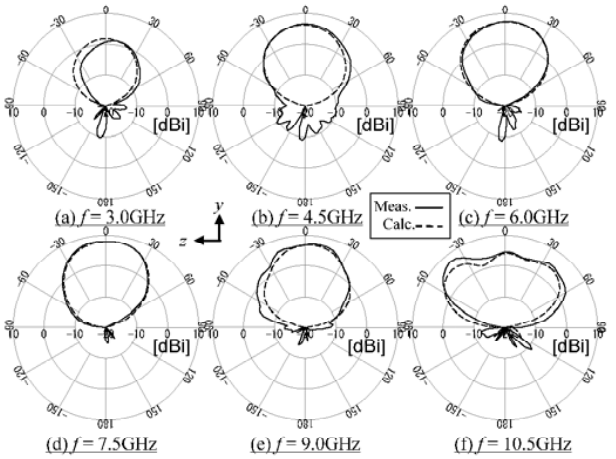

Fig. 5: Radiation patterns in yz plane at the frequency of 3.0, 4.5, 6.0, 7.5, 9.0 and 10.5 GHz.

The measured transmission loss and group delay at $\phi_{\rm rx} = \phi_{\rm tx} = 90^\circ$ are plotted in Figs.6 and 7, respectively. In the

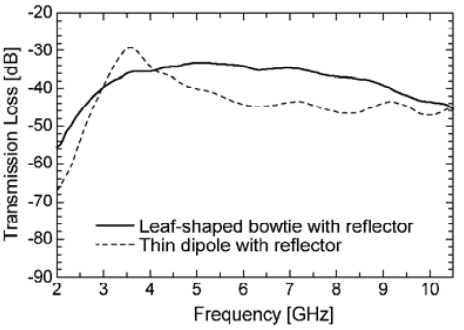

Fig. 6: Transmission loss for the proposed antenna and the MSL thin dipole antenna at $\phi_{\rm tx} = 90^\circ, \phi_{\rm rx} = 90^\circ$.

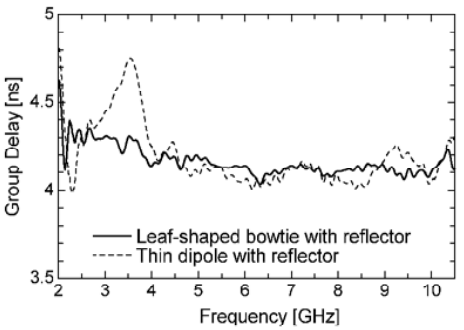

Fig. 7: Group delay for the proposed antenna and the MSL thin dipole antenna at $\phi_{\rm tx} = 90^\circ, \phi_{\rm rx} = 90^\circ$.

case of the proposed antenna, the transmission loss is from -40 up to -33 dB at frequencies of 3–10 GHz. It is observed that the variation in the transmission loss with the frequency is small. For the MSL thin dipole antenna, there is a peak about -30 dB at 3.58 GHz. This is because the MSL thin dipole antenna behaves as a $\lambda/2$ dipole antenna at this frequency and good impedance matching is realized.

The group delay of the proposed antenna is within a band of 4.0–4.3 ns over the frequency range of 3.0 to 10.5 GHz. On the other hand, although the group delay of the MSL thin dipole is within a band of 4.0–4.3 ns in 4.0–10.5 GHz, the peak value of about 4.7 ns is observed at 3.58 GHz in the same way as the transmission loss. As a result, the group delay of the proposed antenna has less frequency variation than that of the MSL thin dipole antenna. Therefore, it is expected that the waveform distortion caused by the proposed antenna is smaller than that caused by the MSL thin dipole antenna.

C. Waveform Distortions

For evaluating waveform distortions caused by the antenna, we need to examine the degree of similarity between source pulse and received pulse waveforms. The degree of similarity between both waveforms can be evaluated in terms of the cross-correlation coefficient between source and received pulses. The cross-correlation coefficient ($CC_{\rm sync}$) can be expressed

as follows:

$$CC_{\mathrm{sync}} = \int_{-\infty}^{+\infty} \hat{s}(t) \cdot \hat{r}(t + \tau_{\mathrm{sync}}) dt \qquad (1)$$

where τ_{sync} is synchronization time, $\hat{r}(t)$ is the normalized received pulse, and $\hat{s}(t)$ is the normalized source pulse. Note that the source pulse and received pulse were assumed to be synchronized in this calculation. The received pulse and the source pulse in the normalized forms are defined as:

$$\hat{r}(t) = \frac{r(t)}{\sqrt{E_r}} = \frac{r(t)}{\sqrt{\int_{-\infty}^{+\infty} r(t)^2 dt}} \qquad (2)$$

$$\hat{s}(t) = \frac{s(t)}{\sqrt{E_s}} = \frac{s(t)}{\sqrt{\int_{-\infty}^{+\infty} s(t)^2 dt}} \qquad (3)$$

where $r(t)$ is the received pulse, $s(t)$ is the source pulse, E_r is the total energy of the received pulse, and E_s is the total energy of the source pulse. The received pulse $r(t)$ is also calculated as:

$$r(t) = \int_{-\infty}^{+\infty} h(\tau) \cdot s(t - \tau) d\tau \qquad (4)$$

where $h(\tau)$ is the impulse response of the propagation channel, which includes the effects of transmitted and received antennas. $h(\tau)$ is obtained by calculating the inverse fourier transformation of the transmission characteristics measured in the previous section. By substituting (2), (3), and (4) into (1), the cross-correlation coefficient (CC_{sync}) can be obtained.

We employed a modulated cosine roll-off pulse[12] as a source pulse $s(t)$, which is defined as:

$$s(t) = \frac{\sin(\pi Bt)}{\pi Bt} \cdot \frac{\cos(\alpha \pi Bt)}{1 - (2\alpha Bt)^2} \cdot \cos(2\pi f_c t) \qquad (5)$$

where α is the roll-off factor, B is the pulse bandwidth, and f_c is the frequency of the modulating wave. In this report, we select the values of $\alpha = 0.25$, $B = 7.5$ GHz, and $f_c = 6.85$ GHz. The time–domain waveform and the power spectrum density (PSD) of the source pulse is shown in Fig.8. The maximum value of the time–domain waveform and the PSD is normalized to 1.0 and 0 dB, respectively. It can be seen from the figure that the PSD of the source pulse covers the UWB band approved by FCC[2].

Calculated correlation coefficients and received energies are shown in Fig.9. In the evaluation, the total energy of the source pulse is normalized to 1 J ($E_s = 1$ J). For the comparison, the results for the antenna without the reflector are also shown in this figure. The proposed antenna has high correlation coefficients of 0.70–0.89 in the range of $\phi_{\mathrm{rx}} = -30°$ to $\phi_{\mathrm{rx}} = 210°$, while the correlation coefficients of the antenna without the reflector range from 0.83 to 0.98. The correlation coefficient at the maximum radiation direction ($\phi_{\mathrm{rx}} = 90°$) deteriorates from 0.96 to 0.72. On the other hand, the correlation coefficients of the MSL thin dipole antenna range from 0.39–0.67. Therefore, the waveform distortion caused by the MSL thin dipole antenna is bigger than that caused by the proposed one. The maximum received energy of the proposed

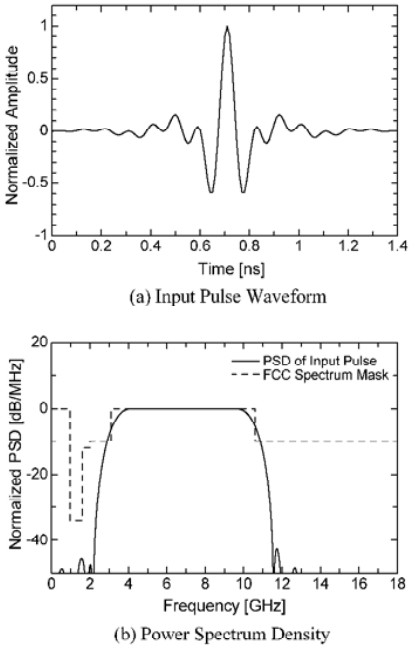

Fig. 8: (a) Time-domain waveform and (b) power spectrum density of the source pulse. The source pulse is a modulated cosine roll-off pulse with parameters f_c =6.85 GHz, B =7.5 GHz, and α =0.25.

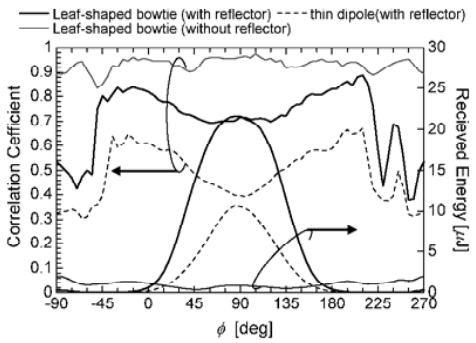

Fig. 9: Correlation coefficient and received energy in azimuthal plane.

antenna is 21.6 μJ, whereas the maximum received energy of the no-reflector antenna is 2.0 μJ. Accordingly, the maximum received energy is improved by 10.2 dB with the use of the reflector.

Fig. 10 shows the time-domain waveform of the source and received pulses at $\phi_{\mathrm{rx}} = 90°$. Note that the received and source pulses are synchronized. For the received pulse of the MSL thin dipole antenna, the obvious ringing is observed at the tail of the waveform. On the other hand, the ringing is very small in the proposed antenna.

4. Conclusion

In this paper, we have proposed a novel bowtie antenna using leaf-shaped radiating elements for UWB applications. The antenna characteristics are investigated by FDTD analysis

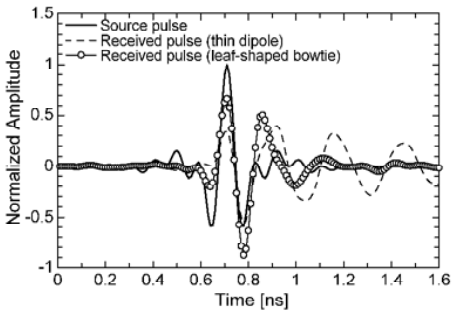

Fig. 10: Time-domain waveform of the source and received pulses.

and measurements. The proposed antenna has the actual gain of 5.0 to 7.2 dBi at the maximum radiation direction over the frequency bandwidth of 4.2 to 10.4 GHz. The radiation patterns are unidirectional and the frequency dependence of the radiation patterns is small in the whole UWB band. In addition, from the measured results of transmission characteristics, the fluctuations in transmission loss and group delay of the proposed antenna are smaller than those of the MSL thin dipole antenna. The correlation coefficient, which is a measure of the degree of the waveform distortions, is between 0.70 and 0.89. Therefore, the waveform distortion caused by this antenna is small. The maximum received energy is improved by 10.2 dB with the use of the reflector. From these results, it is confirmed that the proposed antenna is useful for impulse-based UWB communication systems using correlation detection.

ACKNOWLEDGMENTS

This work was supported by a grant from Japan Society for the Promotion of Science 16760284.

REFERENCES

[1] J. D. Taylor, *Introduction to Ultra-Wideband Radar Systems*, CRC PRESS, Boca Raton, 1995.

[2] FCC, "First Report and Order, Revision of Part 15 of the Commission's Rules Regarding Ultra-Wideband Transmission System," , FCC02-48, Apr. 2002.

[3] H. G. Schantz and M. Barnes, "The COTAB UWB magnetic slot antenna," *IEEE AP-S Int. Symp. Dig.*, Boston, 2001, Vol. 4, pp. 104-107.

[4] H. G. Schantz, "Planar elliptical element ultra-wideband dipole antennas," *IEEE AP-S Int. Symp. Dig.*, San Antonio, 2002, Vol. 3, pp. 44-47.

[5] X. H. Wu and Z. N. Chen, "Comparison of Planar Dipoles in UWB Applications," *IEEE Trans. Antennas Propag.*, Vol. 53, No. 6, 2005, pp. 1973-1983.

[6] Z. N. Chen, "Novel bi-arm rolled monopole for UWB applications," *IEEE Trans. Antennas Propag.*, Vol. 53, No. 2, 2005, pp. 672-677.

[7] M. Ameya, M. Yamamoto, and T. Nojima, "An Omnidirectional UWB Printed Dipole Antenna with Small Waveform Distortion", PIERS2006, Tokyo, 2006.

[8] J. S. McLean, H. Foltz, and R. Sutton, "Pattern Descriptors for UWB Antennas," *IEEE Trans. Antennas Propag.*, Vol. 53, No. 1, 2005, pp. 553-559.

[9] S. Nikolaou, G. E. Ponchak, J. Papapolymerou, and M. M. Tentzeris, "Conformal Double Exponentially Tapered Slot Antenna (DETSA) on LCP for UWB Applications," *IEEE Trans. Antennas Propag.*, Vol. 54, No. 6, 2006, pp. 1663-1669.

[10] Y. Mushiake, *Self-Complementary Antennas: Principle of Self-Complementarity for Constant Impedance*, Springer, 1996.

[11] J. D. Kraus and R. J. Marhefka, *Antennas for All Applications*, McGraw-Hill, New York, 2002.

[12] J. G. Proakis, *Digital Communications, 4th ed.*, McGraw-Hill, New York, 2000.